Phytochemistry xxx (2015) xxx–xxx

Contents lists available at ScienceDirect

Phytochemistry

journal homepage: www.elsevier.com/locate/phytochem

Biochemical characterization of a novel carboxypeptidase inhibitor from a variety of Andean potatoes

Daniela Lufrano [b,1], Juliana Cotabarren [a], Javier Garcia-Pardo [b], Roberto Fernandez-Alvarez [b], Olivia Tort [b], Sebastián Tanco [b,2], Francesc Xavier Avilés [b], Julia Lorenzo [b,*], Walter D. Obregón [a,*]

[a] Laboratorio de Investigación de Proteínas Vegetales, Departamento de Ciencias Biológicas, Facultad de Ciencias Exactas, Universidad Nacional de La Plata, 115 y 47 s/N, B1900AVW La Plata, Argentina

[b] Institut de Biotecnologia i de Biomedicina and Departament de Bioquimica i Biologia Molecular, Universitat Autònoma de Barcelona, Campus Universitari, Bellaterra, Cerdanyola del Vallès, 08193 Barcelona, Spain

ARTICLE INFO

Article history:
Received 27 January 2015
Received in revised form 24 July 2015
Accepted 30 September 2015
Available online xxxx

Keywords:
Andean potatoes
Solanum tuberosum
Solanaceae
Plant protease inhibitor
Potato carboxypeptidase inhibitor
Secondary binding site

ABSTRACT

Natural protease inhibitors of metallocarboxypeptidases are rarely reported. In this work, the cloning, expression and characterization of a proteinaceous inhibitor of the A/B-type metallocarboxypeptidases, naturally occurring in tubers of *Solanum tuberosum*, subsp. *andigenum* cv. Imilla morada, are described. The obtained cDNA encoded a polypeptide of 80 residues, which displayed the features of metallocarboxypeptidase inhibitor precursors from the Potato Carboxypeptidase Inhibitor (PCI) family. The mature polypeptide (39 residues) was named imaPCI and in comparison with the prototype molecule of the family (PCI from *S. tuberosum* subsp. *tuberosum*), its sequence showed one difference at its N-terminus and another three located at the secondary binding site, a region described to contribute to the stabilization of the complex inhibitor-target enzyme. In order to gain insights into the relevance of the secondary binding site in nature, a recombinant form of imaPCI (rimaPCI) having only differences at the secondary binding site with respect to recombinant PCI (rPCI) was cloned and expressed in *Escherichia coli*. The rimaPCI exhibited a molecular mass of 4234.8 Da by MALDI-TOF/MS. It displayed potent inhibitory activity towards A/B-type carboxypeptidases (with a *Ki* in the nanomolar range), albeit 2–4-fold lower inhibitory capacity compared to its counterpart rPCI. This result is in agreement with our bioinformatic analysis, which showed that the main interaction established between the secondary binding site of rPCI and the bovine carboxypeptidase A is likely lost in the case of rimaPCI. These observations reinforce the importance of the secondary binding site of PCI-family members on inhibitory effects towards A/B-type metallocarboxypeptidases. Furthermore, as a simple proof of concept of its applicability in biotechnology and biomedicine, the ability of rimaPCI to protect human epidermal growth factor from C-terminal cleavage and inactivation by carboxypeptidases A and B was demonstrated.

1. Introduction

Proteases (or peptidases) are enzymes that irreversibly cleave proteins by catalyzing peptide-bond hydrolysis. The human genome encodes about 560 proteases that represent around 2% of all human genes, indicating the importance of this class of enzymes (Quesada et al., 2009; Rawlings et al., 2012). Proteases play essential roles in multiple biological processes, and their hydrolytic activities need to be strictly controlled by several mechanisms including the action of specific inhibitors (Turk et al., 2012). One of the main groups of proteases is constituted of metallocarboxypeptidases (MCPs), which hydrolyze the peptide bond at the C-terminus of peptides and proteins by a zinc-dependent mechanism (Fernández et al., 2013; Jozic et al., 2002). MCPs were initially described as pancreatic proteases, but over the years they were found in other locations taking part in a huge variety of

Abbreviations: bCPA, carboxypeptidase A from bovine pancreas; hCPA1, human carboxypeptidase A1; hCPA2, human carboxypeptidase A2; pCPB, carboxypeptidase B from porcine pancreas; DMSO, dimethyl sulfoxide; EGF, epidermal growth factor; imaPCI, Imilia morada Andean Potato Carboxypeptidase Inhibitor; MALDI-TOF/MS, matrix-assisted laser desorption and ionization time-of-flight/mass spectrometry; MPCs, metallocarboxypeptidases; MPCI, metallocarboxypeptidase inhibitor; MS/MS, tandem mass spectrometry; PCI, Potato Carboxypeptidase Inhibitor; PIs, protease inhibitors; PPIs, proteinaceous protease inhibitors; rimaPCI, recombinant imaPCI; rPCI, recombinant PCI; RT-PCR, reverse transcription polymerase chain reaction.

* Corresponding authors.
E-mail addresses: julia.lorenzo@uab.es (J. Lorenzo), davidobregon@biol.unlp.edu.ar (W.D. Obregón).
[1] Permanent address: Laboratorio de Investigación de Proteínas Vegetales, Departamento de Ciencias Biológicas, Facultad de Ciencias Exactas, Universidad Nacional de La Plata, 115 y 47 s/N, B1900AVW La Plata, Argentina.
[2] Present address: Department of Medical Protein Research, VIB, B-9000 Ghent, Belgium. Department of Biochemistry, Ghent University, B-9000 Ghent, Belgium.

http://dx.doi.org/10.1016/j.phytochem.2015.09.010
0031-9422/

physiological processes such as blood coagulation/fibrinolysis, inflammation, prohormone and neuropeptide processing, local anaphylaxis, insect/plant-attack/defense strategies, and growth factors regulation, among others (Arolas et al., 2007; Fernández et al., 2013; Tanco et al., 2013). The dysregulated activity of some MCPs has been associated with several diseases in humans (Fernández et al., 2013); therefore, the use of protease inhibitors (PIs) has emerged as a promising tool in the development of therapeutic strategies for a large number of diseases. Many PIs with pharmacological uses are small molecules obtained by synthetic procedures (Abbenante and Fairlie, 2005; Fear et al., 2007; Fernández et al., 2013); however, natural PIs offer not only a greater chemical diversity and higher specificity, but also lower toxicity and hydrophobicity (Fear et al., 2007). Among natural PIs, the proteinaceous protease inhibitors (PPIs) are especially abundant in the storage organs of some families of the plant kingdom (*e.g.* Solanaceae). One of the most extensively studied PPIs in plants is the Potato Carboxypeptidase Inhibitor (PCI), isolated from tubers of *Solanum tuberosum* subsp. *tuberosum* L. cv. Desirée (Solanaceae), commonly known as the potato. The mature form of PCI is a single polypeptide chain of 39 amino acids stabilized by three disulfide bonds that determine a globular core of 27 residues. This particular conformation situates the PCI among the cystine-knot or T-knot superfamily proteins (Bateman and James, 2011; Bronsoms et al., 2003). From its globular core protrudes a C-terminal tail of five residues (residues 35-39) that is capable of inhibiting the catalytic activity of A/B-type MCPs by mimicking the substrate binding to their active site (Avilés et al., 1993; Marino-Buslje et al., 2000). Once the stable complex is formed, the C-terminal Gly of PCI is cleaved by the enzyme while the rest of the PCI tail remains tightly bound to the MCP's active site, thereby impeding further access of substrates (Arolas et al., 2004; Zhang et al., 2012). Besides the C-terminal tail that constitutes the primary binding site with the enzyme, a secondary surface including residues 15, 23 and 28–31 of PCI has also been proposed to contribute to the efficient interaction of the molecule with its target enzyme (Arolas et al., 2004; Marino-Buslje et al., 2000).

Reported herein is the identification of a novel member of the PCI-family present in *S. tuberosum* L. subsp. *andigenum* cv. Imilla morada, a variety of potato that grows along the Andean Cordillera in South America. The novel inhibitor, named imaPCI, was cloned starting from total RNA isolated from the tuber buds and expressed in *Escherichia coli* for its functional characterization. The recombinant product (rimaPCI) was identified and characterized using proteomic tools and the *Ki* values of rimaPCI and recombinant PCI (rPCI) were determined against four selected A/B-type MCPs. Complementary to the kinetic assays, an *in silico* analysis was performed to further correlate the natural divergence in amino acids that constitute the secondary binding sites of imaPCI and PCI, with their different inhibitory properties. Finally, the ability of imaPCI to protect the epidermal growth factor from C-terminal cleavage and inactivation by MCPs was evaluated, as a simple proof of concept of its applicability in biotechnology and biomedicine. This work expands the current knowledge of PPIs present in potatoes, one of the most cultivated and consumed crops all over the world. Particularly, it paves the way for studying MCP-inhibitors (MCPIs) in Andean potatoes, which thanks to their thousands of varieties represent an extensive reservoir of molecules of huge diversity for biotechnological and pharmaceutical applications.

2. Results

2.1. Cloning and analysis of the cDNA sequence of the imaPCI precursor

In order to identify novel natural MCPIs, total RNA was isolated from tuber buds of the Andean potato Imilla morada variety and a cDNA of 360 bp was obtained by RT-PCR using primers based on conserved regions between the inhibitors of *S. tuberosum* subsp. *tuberosum* L. and *Solanum lycopersicum* L. (Solanaceae). The amplified cDNA was subjected to multiple sequence alignment using the BLAST program (Altschul et al., 1997), revealing a high degree of similarity with sequences of members belonging to the PCI family (inhibitor family I37 in MEROPS database (Rawlings et al., 2014). Particularly, the obtained sequence showed 97% identity (Score value = 603; *E*-value = 6e−169) with *S. tuberosum* metallocarboxypeptidase inhibitor IIa (PCI) precursor mRNA (GenBank: NM_001288119.1). The protein product encoded by 243 bp of the obtained cDNA was named imaPCI precursor and uploaded to the GenBank database under accession number KM359974. The nucleotide and deduced amino acid sequences of the imaPCI precursor are shown in Fig. 1A. The sequence of imaPCI precursor was compared with the amino acid sequence of the PCI precursor (GenPept: NP_001275048.1), in order to identify characteristic regions and residues. The typical organization for the PCI family members (González et al., 2003) was also observed for the imaPCI precursor. That is, a putative signal peptide (only partially amplified through the cloning strategy used in this work), an N-terminal pro-segment of 27 amino acids followed by 39 residues of the mature imaPCI protein, and a 7 residue-extension at the C-terminus (Fig. 1A). Although imaPCI and PCI precursors share 97% nucleotide sequence identity, the mature domains of these inhibitors differ in 4 of the 39 residues (11%) of their primary sequences. As shown in Fig. 1B, most of the non-conserved residues between both sequences (i.e. positions 3, 23, 29 and 30 of the mature protein numbering) are located in positions corresponding to the region known as secondary binding site of these inhibitors (i.e. positions 15, 23 and 28–31), whereas only one amino acid along the rest of the sequences is different, i.e. His3 in PCI and Asp3 in imaPCI. The six conserved cysteine residues, described to be involved in disulfide bond formation (Cys8–Cys24; Cys12–Cys27 and Cys18–Cys34, mature protein numeration) (Chang et al., 1994), are also present in the imaPCI sequence. Moreover, when the amino acid sequence of the mature imaPCI was analyzed by the KNOTER1D tool of the KNOTTIN database software (Gracy et al., 2008), the expected knottin structure was predicted with a knoter1d score of 41 (knottin predictive score > 21). No N-glycosylation or phosphorylation putative sites along the mature imaPCI sequence were predicted by NetNGlyc 1.0 Server (Blom et al., 2004) and NetPhos 2.0 Server (Blom et al., 1999), respectively. An average molecular mass of 4214.7 Da and a pI value of 5.4 were calculated for the mature inhibitor using the Compute pI/Mw tool (Gasteiger et al., 2005). In brief, the imaPCI amino acid sequence shares features described for the members of the MEROPS inhibitor family I37.

2.2. Heterologous expression and purification of rimaPCI

The differences in the secondary binding site are especially interesting since studies based on site-directed mutagenesis and alanine-scanning mutagenesis of recombinant PCI (rPCI), have shown that the secondary binding site of PCI significantly contributes to the stabilization of its inhibitory complex with bCPA (Arolas et al., 2004; Marino-Buslje et al., 2000). Consequently, imaPCI constitutes a natural variant of PCI useful to investigate the importance of the secondary binding site in carboxypeptidase inhibition. For this reason, and for simplicity of the analysis, an imaPCI variant (rimaPCI) was recombinantly produced that maintains the divergences in the secondary binding site, but lacks the differences in its N-terminus with respect to the rPCI sequence (Fig. 2). Interestingly, the N-terminus of rPCI (and therefore also of rimaPCI) corresponds to the reported sequence of isoinhibitor IIa isolated from potato (Hass and Derr, 1979), i.e. a Glu residue

Please cite this article in press as: Lufrano, D., et al. Biochemical characterization of a novel carboxypeptidase inhibitor from a variety of Andean potatoes. Phytochemistry (2015), http://dx.doi.org/10.1016/j.phytochem.2015.09.010

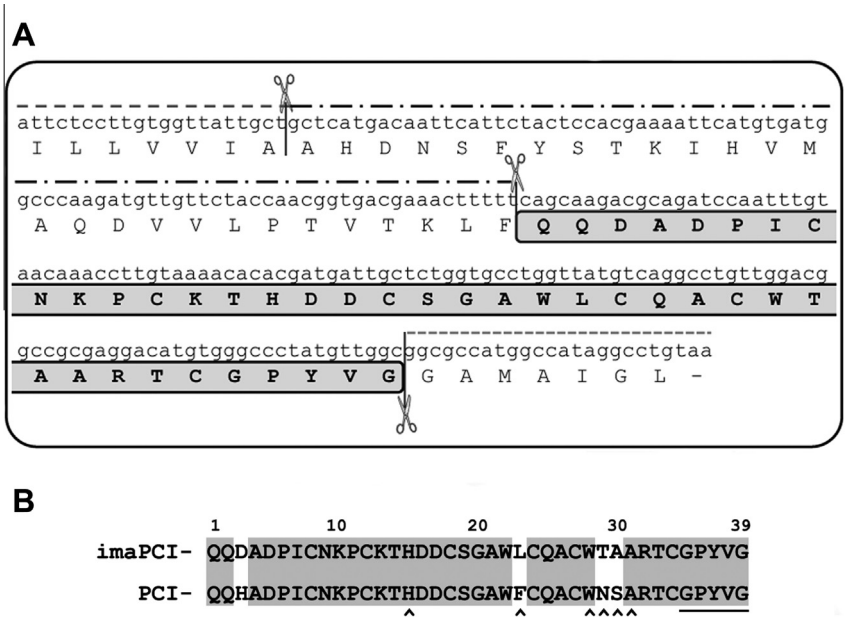

Fig. 1. Nucleotide and deduced amino acid sequences of imaPCI precursor. (A) The cDNA encoding part of the precursor form of imaPCI, a metallo-carboxypeptidase A/B-type inhibitor, was obtained starting from the total RNA isolated from the tuber buds of Imilla morada, a variety of Andean potatoes. The organization of the primary structure is indicated: last portion of the signal peptide (– – -), followed by the N-terminal pro-segment (– · –), the 39-residue mature imaPCI (inside the grey box) and the C-terminal extension of seven amino acids (——). The processing sites for the conversion of the imaPCI precursor into the mature form are indicated by the scissors. (B) Alignment of deduced amino acid sequences of mature imaPCI and PCI (*S. tuberosum*, subsp. *tuberosum*, GenPept: NP_001275048.1), the most similar protein retrieved from the BLAST database. Identical residues are highlighted in gray whereas the divergences between the sequences are represented by white areas. The (^) below the sequences indicate the residues of the inhibitors that together form the secondary binding site to the target enzymes. The inhibitor C-terminal tail (residues 35–39) that interacts with the active site of MCPs is underlined in the figure. The Gly 39 is cleaved by the enzymes and the rest of the tail remains bound to the catalytic pocket impeding further access of substrates.

instead of the Gln deduced from PCI cDNA sequence (Fig. 2), because of the cyclization of the N-terminal Gln to pyroglutamic acid (UniProt: P01075[1]). As previously described in Section 2.4, a three-step PCR strategy was employed for cloning the rimaPCI sequence into the pIN-III vector with the OmpA3 signal peptide sequence on the 5′ end of the rimaPCI gene for achieving periplasmic expression. Upon expression of rimaPCI in *E. coli* BL21 (DE3) strain, the extracellular fraction was collected and submitted to a disulfide bond reshuffling procedure in the presence of cysteine/cystine, in order to generate scrambled species resembling the native structure, as can be followed by RP-HPLC chromatography (data not shown). After reshuffling, the sample was clarified by an overnight incubation at 4 °C and pH 4.0 and then, purified by a procedure specifically optimized for rimaPCI. The clarified sample was applied to the mixed-mode Streamline Direct HST adsorbent. The fractions eluted at a pH value of around 5.0, showing bands of the expected molecular weight in the electrophoretic analysis (indicated in the chromatogram by the shaded area in Fig. 3A), were pooled and adjusted to pH 7.4. Finally, a gel filtration polishing step was performed in a HiLoad 26/60 Superdex 30 prep grade column to obtain the final sample of rimaPCI used for characterization purposes (Fig. 3B).

The rimaPCI showed an electrophoretic mobility similar to that of pure rPCI (4300.7 Da) when analyzed on a 16% Tricine-SDS-polyacrylamide gel under reducing conditions (Fig. 3C). As observed in the RP-HPLC chromatogram shown in Fig. 3D, rimaPCI elutes approximately 2 min later than rPCI from a C4 column, using a 0.66% acetonitrile/min gradient (3–36%) applied for protein elution. This delay in elution indicated that rimaPCI is slightly more hydrophobic than rPCI as would be expected from its less negative GRAVY (grand average of hydropathicity) value (Kyte and Doolittle, 1982; Stothard, 2000), i.e. −0.479 versus −0.644 for rPCI.

The molecular weight for the purified protein product was determined by MALDI-TOF/MS (Fig. 4) and a value of 4234.0 Da was assigned, which is in agreement with the theoretical monoisotopic mass of 4234.8 Da calculated by the Compute pI/Mw tool (Gasteiger et al., 2005). As shown in Fig. 5, the presence of rimaPCI in the purified sample was further confirmed by PMF with sequence coverage of 82% (mass error tolerance: 0.1 Da). Additionally, the peptides with *m*/*z* of 1596.7 Da and 2265.9 Da generated in the PMF (Fig. 5) were selected by the timed-ion-selector. MALDI-TOF/TOF Tandem Mass Spectrometry sequence analysis obtained from the 1596.7 Da peptide allowed us to determine the sequence (EQHADPICNKPCK) that corresponds to the N-terminal amino acids of the rPCI (gi: 159162377) which is also shared by the produced rimaPCI (Supplementary material Fig. S1). In contrast, the analysis of the peptide of 2265.9 Da showed no match with the database rPCI sequence, which is in accordance with the three differences between both sequences (rimaPCI and rPCI) along the fragment 14–32 of the recombinant proteins (Supplementary material Fig. S1).

2.3. Determination of the inhibition kinetic constants (Ki) against A/B-type MCPs

The inhibitory properties of recombinant rimaPCI against four selected A/B-type MCPs were determined and compared with the respective capacities of rPCI. The *K*i values of rimaPCI and rPCI against bCPA, hCPA1, hCPA2 and pCPB were evaluated following a pre-steady-state based protocol, according to the Morrison model for tight-binding inhibitors. All *K*i values determined for rimaPCI (summarized in Table 1) were in the nanomolar range, characteristic of tight-binding inhibitors of MCPs. When compared to rPCI, the *K*i values obtained for rimaPCI against bCPA, hCPA1 and hCPA2 were about 2–2.5-fold lower than the *K*i values obtained for rPCI, and 4-fold lower when pCPB was the target enzyme. These results suggest that the residues Leu23, Thr29 and Ala30 present in rimaPCI (instead of Phe23, Asn29 and Ser30 in rPCI sequence) lead

Please cite this article in press as: Lufrano, D., et al. Biochemical characterization of a novel carboxypeptidase inhibitor from a variety of Andean potatoes. Phytochemistry (2015), http://dx.doi.org/10.1016/j.phytochem.2015.09.010

```
          1         10        20        30        39
PCI-  QQHADPICNKPCKTHDDCSGAWFCQACWNSARTCGPYVG
rPCI- EQHADPICNKPCKTHDDCSGAWFCQACWNSARTCGPYVG
imaPCI-QQDADPICNKPCKTHDDCSGAWLCQACWTAARTCGPYVG
rimaPCI-EQHADPICNKPCKTHDDCSGAWLCQACWTAARTCGPYVG
                          ^         ^    ^^^^
```

Fig. 2. Sequence alignment of mature PCI, imaPCI and their produced recombinant forms. Two mutations were introduced into the cDNA encoding mature imaPCI when the expression construct pIN-III-Omp-A3-rimaPCI was obtained. These mutations changed the N-terminal residues of mature imaPCI to resemble the sequence of rPCI, which has a Glu1 like the native form (PCI) isolated from potatoes (thus instead of Gln1). In the alignment, the sequence of native PCI was used as reference: residues that are identical to the PCI sequence are shadowed in gray, amino acids that differ from PCI are indicated by the white areas, and white letters over a black background represent the mutations introduced into the N-terminal sequence of imaPCI to confine the divergences between rimaPCI and rPCI solely to the secondary binding site (indicated in the figure by the "Λ" below the sequences).

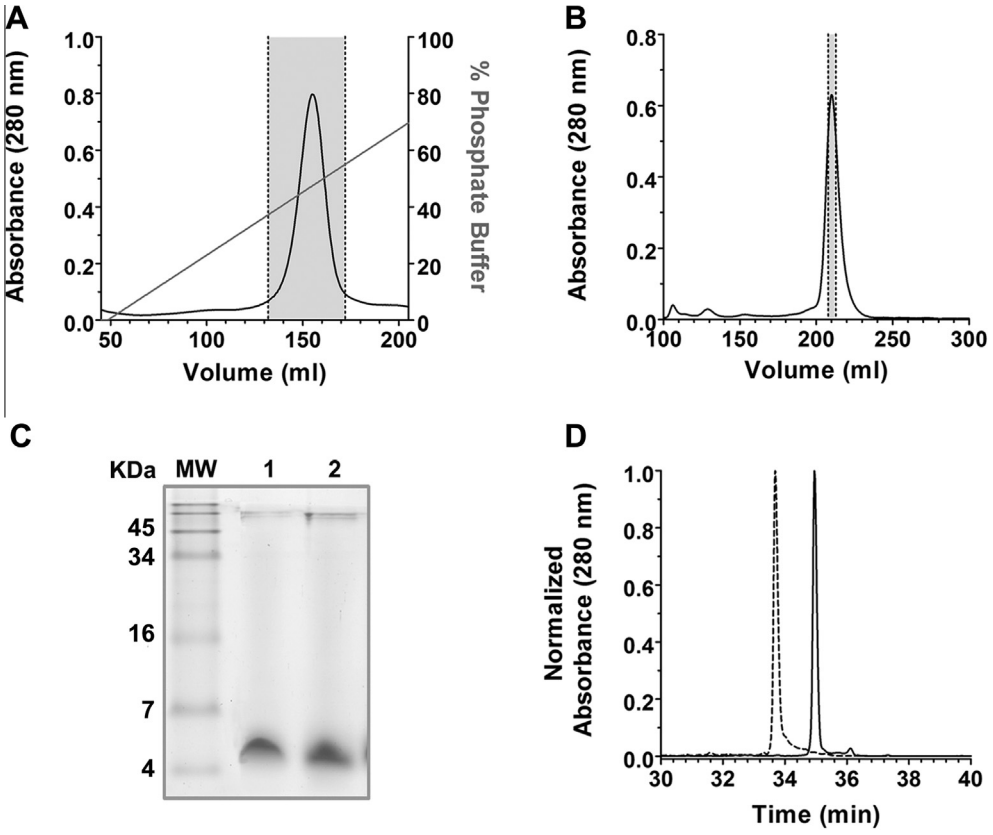

Fig. 3. Purification of rimaPCI. rimaPCI was expressed in *E. coli* and retrieved from the culture media. After a disulfide reshuffling procedure and a clarification step, rimaPCI was purified by a mixed-mode chromatography followed by a gel filtration chromatography. (A) Protein elution profile from Streamline Direct HST adsorbent. Fractions enriched in imaPCI (gray area limited by dotted line in the chromatogram) were pooled and repurified by chromatography. (B) Gel filtration polishing of the mixed-mode chromatography eluate using a HiLoad 26/60 Superdex 30 prep grade column. The collected fraction of rimaPCI is indicated in the chromatogram by the gray area. (C) Tricine-SDS PAGE analysis of purified rimaPCI (7.5 μg); rPCI (7.5 μg) was also loaded in the gel for comparison purposes. Proteins were stained with Coomassie Brillant Blue. (D) RP-HPLC elution profiles of purified rimaPCI (bold line) and rPCI (dotted line).

to an overall decrease in inhibition efficiency against the tested MCPs when compared with rPCI.

2.4. rimaPCI-carboxypeptidase A complex modeling

In the attempt to correlate the differences observed in the *K*i values between rimaPCI and rPCI with the divergences in their sequences, a 3D-structural models of rimaPCI and its complex with bCPA were generated. The rPCI structure is shown in Fig. 6A; the amino acid side-chains of the natural mutations between rPCI and rimaPCI at positions 23, 29 and 30 are represented as an overlap. The 3D model of the rimaPCI-bCPA complex (Fig. 6B) shows the location of the side-chains of the amino acid residues that constitute the secondary binding site of the inhibitor (i.e. His15, Trp22, Leu23, Trp28, Thr29 and Ala30). The surface of bCPA involved in the interaction with the inhibitor secondary binding site is highlighted in the cartoon representation. According to the model, the side-chain of Thr29 remains closer to the Ile247 of bCPA than the Asn29 of rPCI, possibly increasing the interaction between the lateral groups. This effect could then counteract the loss of the capacity to form hydrogen bonds with the Thr246 of bCPA when an Ala residue, instead of a Ser, is situated in position 30. In addition, the presence of a Leu at position 23 might not only abolish the interaction between the aromatic rings of Phe23 of rPCI and Phe279 of bCPA, but it would also reduce the surface of the inhibitor secondary binding site available to make contact with the enzyme.

2.5. Protective effect of rimaPCI on C-terminal proteolysis of peptide growth factors: The EGF case

The ability of rimaPCI to protect proteins with biotechnological and biomedical interest from C-terminal proteolysis was evaluated

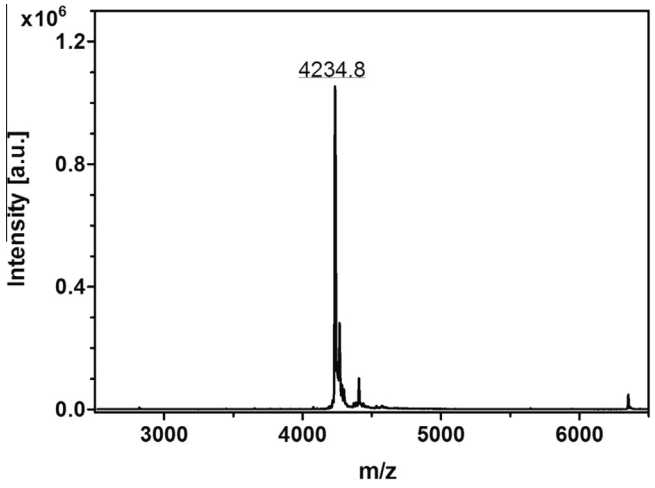

Fig. 4. Maldi-Tof MS analysis of rimaPCI. The MALDI-TOF/MS spectrum of purified rimaPCI is depicted. The peak of the molecular ion (MH^+) showed a monoisotopic mass (m/z) of 4234.8 Da.

using human EGF_{1-53} (Fig. 7A). For this aim, recombinant human EGF_{1-53} was incubated with a mixture of bCPA and pCPB in the absence or presence of rimaPCI for 2 h at 37 °C and pH 7.5. Digestion products were analyzed by MALDI-TOF MS and representative spectra are shown in Fig. 7B–D. Combined action of bCPA and pCPB removed up to six C-terminal residues from EGF_{1-53} molecule, being the major products the forms EGF_{1-47} and EGF_{1-48}. A peak of minor intensity, corresponding to EGF_{1-51} form, was also observed. As can be observed in Fig. 7D, the addition of 100 nM rimaPCI to the reaction mix, had a protective effect against C-terminal hydrolysis of EGF by MCPs by blocking the cleavage of the bound between residues Glu51 and Leu 52.

3. Discussion

It is well known that regulation of proteolysis constitutes a key aspect of physiological processes and healthy state preservation (Abbenante and Fairlie, 2005). The dysregulated activity of some endogenous proteases, as well as the action of pathogen-derived proteases, are involved in several human diseases. More intensively over the last 20 years, the design of therapies based on PIs has gained relevance (*e.g.* for the treatment of human immunodeficiency virus (HIV), hepatitis C, cancer, hypertension, Alzheimer's disease, diabetes mellitus, arthritis, and ischemia (Abbenante and Fairlie, 2005; Fear et al., 2007; Oliva and Sampaio, 2009)). In particular, rPCI shows potential as an anti-malarial agent (Avilés Puigvert et al., 2008) and as an antithrombotic drug (Wang et al., 2006). However, the clinical use of PIs is still facing major problems related with its target selectivity/specificity leading to undesired side–effects, as well as to treatment failure when the target enzyme mutates and develops resistance to the administered PI (Abbenante and Fairlie, 2005). Therefore, the continuous search of new inhibitors to increase the number of clinical candidates constitutes an important challenge. Even with endopeptidase inhibitors being extensively explored (Rawlings et al., 2014), only a limited number of biomolecules able to inhibit metallocarboxypeptidases have been reported so far (Alonso del Rivero et al., 2013).

In this work, a novel member of the PCI family of MCPI naturally occurring in the variety Imilla morada of Andean potatoes is described, and named imaPCI. The sequence of the reported inhibitor was obtained through amplification of the cDNA encoding the precursor form of imaPCI, starting from a total RNA sample and using specific primers. According to the analysis of the deduced amino acid sequence, mature imaPCI displays a high similarity with mature PCI, the most studied proteinaceous MCPI (Arolas et al., 2005; Fernández et al., 2013). Both inhibitors possess the same residues at the C-terminal tail (including the C-terminal Gly), indicating a conserved mechanism of inhibition of A/B-type MCPs; however, they present differences in three of the six residues that constitute the secondary interacting surface with the target MCPs (Arolas et al., 2005,2004; Marino-Buslje et al., 2000). Because the secondary binding site of PCI is described to significantly contribute to stabilizing the complex with the target enzyme (Marino-Buslje et al., 2000), a recombinant form of mature imaPCI was produced in *E. coli*. This recombinant form of imaPCI, termed rimaPCI, acts as a natural triple mutant (F23L, N29T, S30A) of the rPCI in order to specifically investigate the importance of the secondary binding site (see Fig. 2 for clarity).

Based on our data, rimaPCI is a biologically active tight-binding inhibitor of A/B-type MCPs; however, the higher *Ki* values obtained indicate a lower inhibitory capacity of rimaPCI compared to rPCI. This result is in agreement with the observations reported by Arolas and co-workers who produced the individual mutant of each amino acid residue participating in the secondary binding site of rPCI (H15A, W22A, F23A, W28A, N29A, S30A, N29G) as well as, two double mutants (F23A/W28A and N29A/S30A) (Arolas et al., 2004). The alanine-scanning mutagenesis approach allowed the authors to conclude that aromatic groups, and not polar lateral chains, are more relevant in the stabilization of the rPCI-bCPA complex. Particularly, they described Phe23 as the most influential residue not only due to the π–π type interaction established with the Phe279 aromatic ring of CPA, but also because of its contribution to the contact interface involved in the complex formation.

A

Experimental PMF (*m/z*)	Theoretical PMF (*m/z*)	Fragment position	Peptide fragment sequence
1596.743	1596.726	1 - 13	EQHADPICNKPCK (2 * Carbamidomethyl (C))
2265.943	2265.922	14 - 32	THDDCSGAWLCQACWTAAR(3 * Carbamidomethyl (C))

B

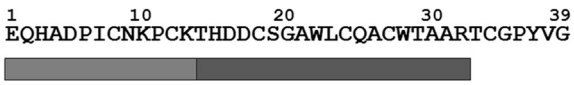

Fig. 5. PMF identification of rimaPCI. The electrophoretic band of ~4.2 kDa corresponding to the purified rimaPCI was submitted to *in situ* tryptic digestion and the resulting peptides were analyzed by MALDI-TOF/MS. (A) Identification of trypsin-digested peptides of rimaPCI by comparison with theoretical PMF. (B) The peptide sequence considered in protein analysis. Bars below the sequence indicate the identified fragments and the spectral peaks intensity (in grayscale).

Please cite this article in press as: Lufrano, D., et al. Biochemical characterization of a novel carboxypeptidase inhibitor from a variety of Andean potatoes. Phytochemistry (2015), http://dx.doi.org/10.1016/j.phytochem.2015.09.010

Table 1
Inhibition kinetic constants (*Ki*) of rPCI and rimaPCI for bCPA, hCPA1, hCPA2 and pCPB.

Enzyme	rPCI	rimaPCI
	Ki (nM)	*Ki* (nM)
bCPA[a]	1.60 ± 0.29	4.05 ± 0.29
hCPA1[a]	0.73 ± 0.09	1.71 ± 0.48
hCPA2[a]	5.30 ± 0.66	14.40 ± 4.20
pCPB[b]	2.40 ± 0.24	9.81 ± 2.90

[a] Measurements were carried using the synthetic substrate *N*-(4-methoxyphenylazoformyl)-Phe-OH.
[b] Measurements were carried using the synthetic substrate *N*-(4-methoxyphenylazoformyl)-Arg-OH.

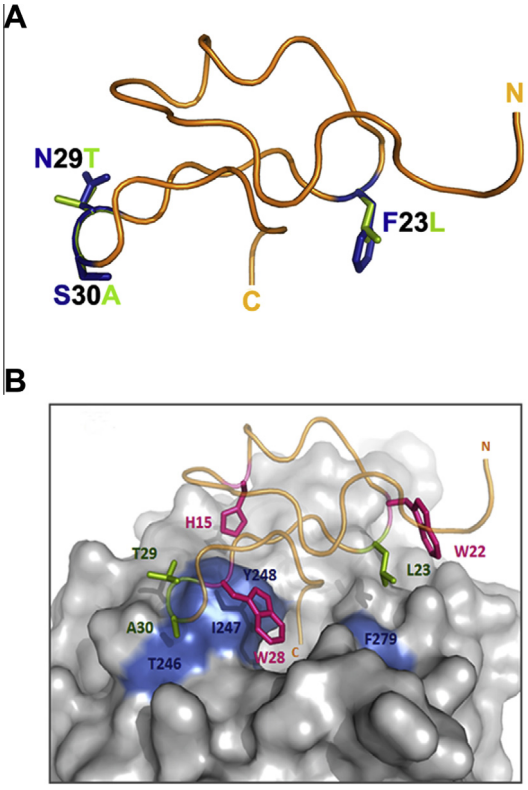

Fig. 6. Schematic surface representation of bCPA in the complex with rimaPCI. (A) Superposition of three dimensional structures of rPCI and rimaPCI showing the locations of differential residues found in the secondary binding site of rimaPCI. Side chains of Phe23, Asp29 and Ser30 of rPCI are depicted in blue, and Leu23, Thr29 and Ala30 residues of imaPCI are shown in green. N and C indicate the N terminus and the C terminus, respectively. (B) 3D model of the rimaPCI-bCPA complex. The locations of the secondary binding residues of the inhibitor (His15, Leu23, Thr29, Ala30 and Trp28) in the complex are indicated in the picture. The positions of the rimaPCI secondary binding site that show differences with the rPCI sequence are represented in green. Residues of bCPA involved in the rimaPCI binding are colored in blue at the enzyme surface (Thr246, Ile247, Tyr248 and Phe279). The protein data bank for the structure of rPCI is 4CPA (Rees and Lipscomb, 1982). All figures were prepared with PyMOL (DeLano, 2002).

Therefore, the drop in the *Ki* values of rimaPCI in comparison with the ones obtained for rPCI could be due mainly to the absence of the Phe23 in rimaPCI with the concomitant loss of the π–π type interaction. Moreover, their (F23A)PCI mutant has a *Ki* towards bCPA about 5-fold higher than what was observed here for rimaPCI, suggesting that replacing Phe by a Leu in position 23 is less dramatic for the inhibitory capacity than a change by an Ala in that position. Probably, the intermediate hydrophobic nature of Leu, which has an individual average area buried (AAB) value between Phe and Ala (i.e., the AAB values are 194.1 for Phe, 164.0 for Leu and 86.6 for Ala), is responsible for the intermediate *Ki* value towards bCPA of rimaPCI in comparison to the values displayed by wild-type rPCI and (F23A)PCI (Arolas et al., 2005; Rose et al., 1985; Stothard, 2000). Also, the difference in the inhibitory effect between rimaPCI and rPCI was approximately the same (~2.5-fold) for the three A-type MCPs tested in this work. Noteworthy, the difference in *Ki* was more pronounced when pCPB inhibition was measured, i.e. rimaPCI was about ~4-fold less potent than rPCI.

Through the identification of a novel inhibitor, the relevance of the secondary contacting region of tight-binding inhibitors belonging to the PCI-family for their inhibitory capacity towards A/B-type MCPs is confirmed. The occurrence of inhibitors showing divergences concentrated in the amino acids of the secondary binding site in two phylogenetically very close plants, also suggests that probably multiple variants of a same inhibitor with slightly different inhibitory capacities co-exist in a single potato subspecies. Furthermore, it could be hypothesized that in nature, this multiplicity might constitute a tool against the inhibitor-resistant mechanism of MCPs developed by some plant predatory species (Zhang et al., 2012). These observations also contribute useful information for the rational design of PCI-like products with diverse inhibitory capacities, to deal with the limitations of PIs for therapeutic and biotechnological applications, (Fischer et al., 2014).

Finally, as an applicative example, rimaPCI showed a protective effect on mature human epidermal growth factor (EGF_{1-53}) from its C-terminal proteolysis by both bCPA and pCPB The binding of the mature EGF_{1-53} to the EGF receptor (EGFR) leads to cell proliferation and wound healing *in vitro* and *in vivo* (Berlanga-Acosta et al., 2009). However, it has been reported that sequential loss of C-terminal amino acids from the EGF molecule by proteolysis (EGF_{1-52}, EGF_{1-51}, EGF_{1-50}, etc.) progressively reduces its biological activity (Goodlad et al., 1996; Gregory et al., 1988; Playford et al., 1995). Even more, the scission of the last 8 amino acids (EGF_{1-45}) can lead to a potent EGFR inhibitor (Panosa et al., 2013). These results for the first time establish the possible usefulness of proteinaceous inhibitors, like rimaPCI, for growth factors protection.

4. Concluding Remarks

A novel proteinaceous inhibitor precursor of metallocarboxypeptidases of the A/B subfamily, denominated imaPCI precursor, was cloned from tubers of *S. tuberosum*, subsp. *andigenum* cv. Imilla morada. The cDNA-deduced amino acid sequence displayed the typical primary structure and domain organization of MCPI precursors belonging to the PCI-family. In comparison with PCI, imaPCI displayed sequence identity in the C-terminus involved in the mechanism of enzyme inhibition. However, both proteins showed divergences in the secondary contacting interface involved in the stabilization of the complex formed with the target enzymes. A recombinant form of imaPCI, rimaPCI, containing only the differences in the secondary binding site in respect to rPCI was then produced in *E. coli*. The produced rimaPCI showed higher inhibitory constants (*Ki*) against A/B-type MCPs than rPCI in the assays, validating a significant contribution of the secondary binding site to the inhibitory capacity of PCI family members towards A/B-type MCPs. As a preliminary study, the potential role of rimaPCI to protect growth factors was demonstrated, taking as example the EGF which C-terminal amino acids are essential for its biological activity.

5. Experimental

5.1. Plant material

Tubers of *S. tuberosum* L., subsp. *andigenum* cv. Imilla morada (Dimitri, 1987) from the province of Jujuy, Argentina, were kept

Please cite this article in press as: Lufrano, D., et al. Biochemical characterization of a novel carboxypeptidase inhibitor from a variety of Andean potatoes. Phytochemistry (2015), http://dx.doi.org/10.1016/j.phytochem.2015.09.010

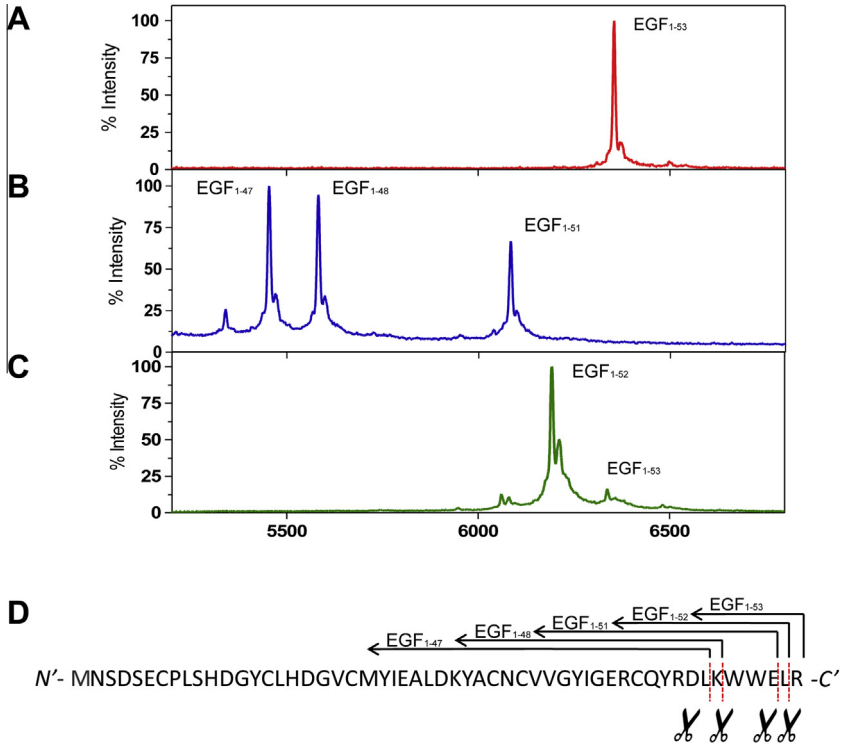

Fig. 7. Proteomic analysis of the human EGF C-terminal proteolysis in the presence of rimaPCI. Representative MALDI-TOF spectra of recombinant full-length EGF (EGF_{1-53}) after incubation in (A) absence or (B) presence of a mixture of 30 nM bCPA and 50 nM pCPB. (C) Representative spectrum of the EGF_{1-53} incubated with bCPA and pCPB in presence of 100 nM rimaPCI. (D) Human EGF_{1-53} amino acid sequence. The peptide bonds cut by the combined action of bCPA and pCPB to produce the main truncated forms, observed in the spectra, are indicated on the sequence. Note that the full-length recombinant human EGF used (purchased from R&D systems) contains the EGF_{1-53} sequence and an additional N-terminal Met residue. Thus, the monoisotopic masses were: EGF_{1-53} = 6348.77; EGF_{1-51} = 6078.85; EGF_{1-48} = 5577.32; EGF_{1-47} = 5449.15.

at room temperature in darkness until ~1 cm buds were grown at the tuber surface.

5.2. Materials

E. coli BL21 (DE3) strain was purchased from Novagen (U.S.A.). pGEM-T Easy vector was obtained from Promega Corporation (U.S.A.). Primers were synthesized by Invitrogen Corporation (U.S.A.). DNA Taq polymerase was purchased from Biotools B&M Labs, S.A. (Spain). Restriction enzymes and DNA ladders were obtained from Roche Applied Science (Germany). DNA T4-ligase was supplied by New England BioLabs (UK). Pre-stained broad range molecular mass standard was purchased from Invitrogen Corporation. Carboxypeptidase A (CPA) and carboxypeptidase B (CPB) from bovine and porcine pancreas, respectively, were supplied by Sigma-Aldrich (U.S.A.). Recombinant PCI, human CPA1 and CPA2 were produced and purified as described previously (Arolas et al., 2004; García-Sáez et al., 1997; Pallarès et al., 2008; Tanco et al., 2010). N-(4-methoxyphenylazoformyl)-phenylalanine-OH potassium salt and N-(4-methoxyphenylazoformyl)-arginine-OH potassium salt were obtained from Bachem (Switzerland). Bacto™ Casamino Acids was purchased from BD (U.S.A). Recombinant human EGF_{1-53} was obtained form R&D Systems (U.S.A.). Other reagents used were of the highest grade available.

5.3. Cloning and sequence analysis

Total RNA was extracted from tuber buds of *S. tuberosum* L., subsp. *andigenum* cv. Imilla morada. Frozen samples (100 mg) were ground in a mortar for appropriate tissue dissection and RNA isolation was carried out using the RNeasy Plant Mini Kit (Qiagen, Germany) according to the manufacturer's instructions. First-strand cDNA was synthesized from an aliquot of total RNA previously treated with DNase I (Thermo, U.S.A), using $R_oR_1$poli $(dT)_{15}$ primer (5′-CCGGAATTCACTGCAGGGTACCCAATACGACTCAC-TATAGGGCTTTTTTTTTTTTTTTT-3′) and Revert Aid First Strand cDNA Synthesis Kit (Thermo). The total cDNA was used as template in a PCR reaction for the amplification of open reading frames (ORFs) corresponding to a part of a MCPI precursor. Primers were specifically designed for conserved regions between cDNAs encoding carboxypeptidase inhibitor precursors in *S. tuberosum* subsp. *tuberosum* L. (GenBank: NM_001288119.1) and *S. lycopersicum* L. (GenBank: NM_001247005.2), (Fwd: 5′-ATTCTCCTTGTGGT-TATTGCTGC-3′ and Rev: 5′-GCCACAAAGCATGTATCTAAGAC-3′). The PCR products were analyzed by 1.5% agarose gel electrophoresis and the resulting amplification fragment of approximately 360 bp was purified and subsequently cloned into pGEM-T Easy vector (Promega). The resulting construct was named pGEM_imaPCIprecursor (accession number: KM359974). Ten positives clones identified by color screening on indicator plates, were submitted to automatic DNA sequencing (Macrogen Inc., Korea).

5.4. Expression of recombinant metallocarboxypeptidase inhibitor

The construct pIN-III-Omp-A3-rimaPCI used for the expression of rimaPCI was obtained by three sequential PCR reactions. This strategy allowed the sequence of the OmpA3 secretion signal to be fused to the mature imaPCI cDNA at the time when two punctual mutations were introduced into the N-terminus of the inhibitor. To carry out this strategy, four primers were specifically designed, three forward (Fwd_1, Fwd_2 and Fwd_3) and one reverse (Rev). In the first PCR, the pGEM-imaPCIprecursor construct was used as a template together with the primer Fwd_1, including the punctual mutations and the sequence encoding the C-terminal portion of

OmpA3, and the primer Rev which introduced an EcoRI restriction site. The primer Fwd_1 was: 5′-CTACCGTAGCGCAGGCCGAACAG-CACGCGGATCCAATTTGTAACAAACCTTGTA-3′, where the double underlined part indicates the sequence corresponding to the N-terminus of mature imaPCI and the bold bases indicate the punctual mutations. The primer Rev was: 5′-GTCAgaattcCTAGCCAACA-TAGGGCCCACATG-3′, where the lower-case letters indicates the EcoRI site. The product of this first PCR was the template used in the following reaction with the primer Fwd_2 and once more, the primer Rev. The primer Fwd_2 introduced the middle part of the OmpA3 sequence: 5′-GCTATCGCGATTGCAGTGGCACTGGCTGGTTT-CGCTACCGTAGCGCAGGCC-3′. The last PCR step was performed with the primer Rev in combination with the primer Fwd_3, which added to the previous amplicon the sequence encoding the N-terminal domain of the OmpA3 and a recognition site for XbaI. The primer Fwd_3 was: 5′-tctagaTAACGAGGGCAAAAAATGAAAAAGACAGCTA-TCGCGATTGCAGTGGC-3′, where the dotted line indicates the part of the OmpA3 sequence, the single solid line indicates the 5′ adjacent region of pIN-III vector and lower-case letters represent the XbaI site. After the third PCR, the final product was submitted to a double digestion with EcoRI and XbaI enzymes and gel purified. The purified fragment of approximately 210 bp was ligated to the expression vector pIN-III (previously digested with the same restriction enzymes), followed by the transformation of the ligation product into the *E. coli* strain TOP10F′ cells. The transformed cells were plated on Luria Bertani (LB) agar containing 0.1 mg/ml ampicillin for growth selection. The isolated colonies were used for plasmid DNA extraction and analyzed by DNA sequencing.

A culture of *E. coli* BL21 (DE3) strain (Novagen) transformed with the pIN-III-OmpA3-rimaPCI construct, was grown overnight at 37 °C in LB medium containing 0.1 mg/ml ampicillin. On the following day, an aliquot of this culture (10 ml) was inoculated into fresh BAT broth (1 l, with minimal media containing 0.51 M Na_2HPO_4, 0.22 M KH_2PO_4, 0.18 M NH_4Cl, 0.085 M NaCl, 0.001 M $MgSO_4$, 3×10^{-4} M $CaCl_2$, 0.001 M Tiamine, 0.5% glycerol, 0.2% casamino acids, 1.4×10^{-4} M $FeSO_4$, 6×10^{-4} M $MnSO_4$, 1.5×10^{-5} $CoCl_4$, 6.9×10^{-6} M $ZnSO_4$, 4.7×10^{-6} M Na_2MoO_4, 1.8×10^{-6} M $CuCl_2$, 7.5×10^{-6} M $AlCl_3$ and 8.1×10^{-6} M H_3BO_3, pH 7.2) with 0.1 mg/ml ampicillin and then allowed to grow at 37 °C until the absorbance at 600 nm reached 0.6. Protein expression was induced by adding 0.2 mM IPTG to the medium and after 20 h of expression at 37 °C, the supernatant containing the recombinant protein was collected by centrifugation at 11,300*g* for 20 min at 4 °C. A disulfide reshuffling procedure, based on the method of Chang modified (Lian et al., 2003), was performed as follows: cysteine (4 mM final concentration) and cystine (2 mM final concentration) was added to the supernatant and pH was adjusted to a value of 8.5, followed by incubation at room temperature for 3 h.

5.5. Purification of rimaPCI

Prior to chromatographic purification, the sample was clarified by adjusting the pH to a value of 4.0 using 1 M citric acid and incubating overnight at 4 °C. After centrifugation at 11,300*g* for 20 min, the supernatant was loaded onto a column containing the mixed-mode adsorbent with cationic exchange ligand Streamline Direct HST (GE Healthcare Biosciences, Sweden), connected to an ÄKTA Purifier FPLC system (GE Healthcare) previously equilibrated with 100 mM sodium citrate buffer (pH 4.0). After a washing step with 100 mM sodium citrate buffer, elution of bound proteins was carried out with a linear gradient of 100 mM sodium phosphate buffer of pH 8.5, thus generating a pH-gradient (from pH 4.0 to pH 8.5). The collected fractions were analyzed by Tricine-SDS-PAGE (Schägger, 2006), and those showing bands of the expected apparent molecular weight were pooled. The pH of the pooled fractions was adjusted to a value of 7.4 and then the sample was concentrated 16-fold in a centrifugal filter device (Amicon Ultra-15 3 K, Millipore, Germany). The concentrated sample was analyzed by RP-HPLC and further purified by gel filtration chromatography employing a HiLoad 26/60 Superdex 30 prep grade column (GE Healthcare) adapted to an ÄKTA Purifier 10 system (GE Healthcare Life Sciences). The pre-equilibration step and the elution of proteins from the Superdex 30 prep grade column were performed with phosphate saline buffer (PBS) at a flow rate of 2.5 mL/min. The concentration of the eluted rimaPCI was estimated by absorbance at 280 nm using its theoretical extinction coefficient (12,865 M^{-1} cm^{-1}) obtained from the ProtParam software (Gasteiger et al., 2005).

5.6. RP-HPLC analysis

A sample containing protein (7.5 μg) was injected onto a C4-column (250 × 4.6 mm, Phenomenex, Germany) connected to an Alliance HPLC system (Waters, U.S.A). Elution was carried out by a linear gradient of CH_3CN: 0.1% CF_3CO_2H (v/v) (3:97–36:64) at a flow rate of 0.75 ml/min over 50 min. The absorbance at 214 nm and 280 nm was continuously monitored during chromatography. For comparative purposes, rPCI was also analyzed under the same conditions.

5.7. Inhibition constants (Ki) determination

The K_i values of rimaPCI and rPCI for the inhibition of four A/B-type MCPs (bCPA, hCPA1, hCPA2 and pCPB) were determined according to the Morrison model for tight-binding inhibitors (Morrison, 1982). Briefly, a fixed concentration of the tested enzyme (2.4 nM of bCPA, 3 nM of hCPA1, 7.4 of nM hCPA2 and 3 nM of pCPB) was pre-incubated in buffer with different concentrations of inhibitor at room temperature. After 10 min, the corresponding chromogenic substrate was added to the reaction mix and, immediately, the absorbance at 340 nm was measured every minute for a minimum of 10 min. Assays were carried out in 20 mM Tris–HCl buffer (pH 7.5) containing 1% v/v DMSO, 0.05% w/v Brij-35 and 500 mM NaCl (for A-like MCPs) or 100 mM NaCl (for B-like MCPs). *N*-(4-methoxyphenylazoformyl)-Phe-OH and *N*-(4-methoxyphenylazoformyl)-Arg-OH were used as substrates at a concentration of 0.1 mM for pCPA and pCPB, respectively. Measurements were carried out in triplicate. Substrate consumption along the assay was about 10% in all cases.

5.8. Proteomic identification of purified inhibitor

5.8.1. Mass spectrometry analysis

Matrix-Assisted Laser Desorption and Ionization Time-of-Flight Mass Spectrometry (MALDI-TOF/MS) was used for the determination of rimaPCI molecular mass. MALDI-TOF mass spectra was acquired on a BRUKER Ultraflex spectrometer equipped with a pulsed nitrogen laser (337 nm), in linear positive ion mode, using a 19 kV acceleration voltage. Samples were prepared by mixing equal volumes of a saturated solution of matrix (3.5-dimethoxy-4-hydroxycinnamic acid) in 0.1% CF_3CO_2H (v/v) in H_2O:CH_3CN (2:1), and 1 μM protein solution. From this mixture, 1 μl was spotted onto the sample slide (MP 384 Polished Steel, Bruker) and allowed to evaporate to dryness at room temperature. The calibration standard mixture consisted of insulin $[M+H]^+$ (*m*/*z* 5734.51), ubiquitin $[M+H]^+$ (*m*/*z* 8565.76), cytochrome C $[M+H]^+$ (*m*/*z* 12360.97), myoglobin $[M+H]^+$ (*m*/*z* 16952.30), cytochrome C $[M+2H]^{2+}$ (*m*/*z* 6180.99), myoglobin $[M+2H]^{2+}$ (*m*/*z* 8476.65), respectively.

Please cite this article in press as: Lufrano, D., et al. Biochemical characterization of a novel carboxypeptidase inhibitor from a variety of Andean potatoes. Phytochemistry (2015), http://dx.doi.org/10.1016/j.phytochem.2015.09.010

5.8.2. Peptide mass fingerprinting by MALDI-TOF/MS

Purified recombinant inhibitor was analyzed by Peptide Mass Fingerprinting (PMF). *In situ* tryptic digestion of an electrophoretically homogeneous band was performed following the protocol of (Obregon et al., 2009). The peptides were dissolved in 5 µl 0.1% CF_3CO_2H (v/ v) and analyzed by MALDI-TOF/MS using a matrix of α-cyano-4-hydroxycinnamic acid (HCCA). Peptide masses were acquired with Flex Control Software in a range of ca. 1000–3500 *m*/*z*. External calibration was performed using a peptide calibration mixture composed of bradykinin [1–7 $[M+H]^+$ (*m*/*z* 757.39916)], angiotensin II $[M+H]^+$ (*m*/*z* 1046.5418), angiotensin I $[M+H]^+$ (*m*/*z* 1296.6848), substance P $[M+H]^+$ (*m*/*z* 1347.7354), bombesin $[M+H]^+$ (*m*/*z* 1619.8223), renin substrate $[M+H]^+$ (*m*/*z* 1758.93261), ACTH clip [1–17 $[M+H]^+$ (*m*/*z* 2093.0862)], ACTH clip [18–39 $[M+H]^+$ (*m*/*z* 2,465.1983)] and somatostatin 28 $[M+H]^+$ (*m*/*z* 3147.4710). The results were processed using the MASCOT search engine (http://www.matrixscience.com). Search parameters were (1) type of search, peptide mass fingerprint; (2) enzyme, trypsin; (3) database, SwissProt 55.2; (4) taxonomy, Viridiplantae; (5) variable modifications, carbamidomethyl (C), oxidation (M); (6) mass values, monoisotopic; (7) peptide mass tolerance,±100 ppm; (8) peptide charge state, 1+. Additionally, the sequence deduced from rimaPCI cDNA was subjected to a theoretical tryptic digestion by means of Sequence Editor 3.1 software (BrukerDaltonics, Biotools 3.1) and compared with the experimental PMF obtained for rimaPCI.

5.8.3. Sequencing by MALDI-TOF/TOF Tandem Mass Spectrometry

For MS/MS, ions generated by the PMF-MALDI-TOF/MS process were accelerated at 8 kV through a grid at 6.7 kV into a short, linear, field-free drift region. In this region, the ions pass through a timed-ion-selector device that is able to select one peptide from a mixture of peptides at different *m*/*z* values for subsequent fragmentation in the collision cell. After a peptide at a given *m*/*z* was selected by the timed-ion-selector, it passed through a retarding lens where the ions were decelerated and then passed into the collision cell, which was operated at 7 kV. Fragmentation was performed in the simple metastable decomposition mode (no collision gas and with the collision energy set at 1 keV).

5.9. rimaPCI-carboxypeptidase A complex modeling

Sequence alignment between rPCI (UniProt P01075) and rimaPCI was generated by using the ClustalW online tool (Larkin et al., 2007). Three-dimensional (3D) structures of rPCI, rimaPCI and the rimaPCI-CPA complex were prepared using a previously solved structure of CPA, with the accession code 4CPA (Rees and Lipscomb, 1982) from the Protein Data Bank (www.rcsb.org) as reference. The rimaPCI 3D-structure was approximated by performing single-residue mutations (N29T, S30A and F23L) at the PCI structure with PyMOL (DeLano, 2002). PyMOL was used for generation and inspection of the models.

5.10. Inhibitory assays of EGF C-terminal proteolysis by rimaPCI

Recombinant human EGF_{1-53} (2.5 µg, R&D Systems) was incubated with 30 nM bCPA and 50 nM pCPB in the absence or presence of 100 nM rimaPCI for 2 h at 37 °C in 20 mM Tris-HCl buffer (pH 7.5) containing 250 mM NaCl. After incubation, reactions were stopped by addition of an equal volume (20 µl) of 0.1% TFA in water, and then, samples were prepared and subjected to MALDI-TOF/MS analysis as described in Section 5.8.1.

Acknowledgements

W.D. Obregón is a member of the Researcher Career Program of the Argentine Council of Scientific and Technical Research (CONICET); D. Lufrano has a postdoctoral fellowship from CONICET. The authors acknowledge support of the Ministerio de Economía y Competitividad (MINECO) of Spain (project BIO2013-44973-R), CONICET (PIP 0120), Universidad Nacional de La Plata (UNLP, PPID X/004) and Bilateral Cooperation Program MinCyT-MICINN (project ES/09/24-AR2009/006). W. D. Obregón and D. Lufrano are grateful to CONICET and UNLP for the mobility grants. Proteomic based assays were carried out in the Proteomics and Bioinformatics Facility of the Universitat Autònoma de Barcelona (SePBioEs-UAB), Barcelona, Spain. SePBioEs is member of the ProteoRed-ISCIII network. The authors also thank A. Nikolaou for the English revision of this paper.

Appendix A. Supplementary data

Supplementary data associated with this article can be found, in the online version, at http://dx.doi.org/10.1016/j.phytochem.2015.09.010.

References

Abbenante, G., Fairlie, D.P., 2005. Protease inhibitors in the clinic. Med. Chem. 1, 71–104.

Alonso del Rivero, M., Reytor, M.L., Trejo, S.A., Chávez, M.A., Avilés, F.X., Reverter, D., 2013. A noncanonical mechanism of carboxypeptidase inhibition revealed by the crystal structure of the Tri-Kunitz SmCI in complex with human CPA4. Structure 21, 1118–1126.

Altschul, S.F., Madden, T.L., Schäffer, A.A., Zhang, J., Zhang, Z., Miller, W., Lipman, D.J., 1997. Gapped BLAST and PSI-BLAST: a new generation of protein database search programs. Nucleic Acids Res. 25, 3389–3402.

Arolas, J.L., Lorenzo, J., Rovira, A., Vendrell, J., Aviles, F.X., Ventura, S., 2004. Secondary binding site of the potato carboxypeptidase inhibitor. Contribution to its structure, folding, and biological properties. Biochemistry 43, 7973–7982.

Arolas, J.L., Lorenzo, J., Rovira, A., Castellà, J., Aviles, F.X., Sommerhoff, C.P., 2005. A carboxypeptidase inhibitor from the tick *Rhipicephalus bursa*: isolation, cDNA cloning, recombinant expression, and characterization. J. Biol. Chem. 280, 3441–3448.

Arolas, J.L., Vendrell, J., Aviles, F.X., Fricker, L.D., 2007. Metallocarboxypeptidases: emerging drug targets in biomedicine. Curr. Pharm. Des. 13, 349–366.

Avilés, F.X., Vendrell, J., Guasch, A., Coll, M., Huber, R., 1993. Advances in metallocarboxypeptidases. Eur. J. Biochem. 211, 381–389.

Avilés Puigvert, F.X., Lorenzo Rivera, J., Rodríguez-Vera, M., Querol Murillo, E., Bautista Marugán, M., Díez Martin, A., Bautista Santa Cruz, J.M., 2008. Therapeutic agents for treatment of malaria. WO2008077977 A1.

Bateman, K., James, M., 2011. Plant protein proteinase inhibitors: structure and mechanism of inhibition. Curr. Protein Pept. Sci. 12, 341–347.

Berlanga-Acosta, J., Gavilondo-Cowley, J., López-Saura, P., González-López, T., Castro-Santana, M.D., López-Mola, E., Guillén-Nieto, G., Herrera-Martinez, L., 2009. Epidermal growth factor in clinical practice – a review of its biological actions, clinical indications and safety implications. Int. Wound J. 6, 331–346.

Blom, N., Gammeltoft, S., Brunak, S., 1999. Sequence and structure-based prediction of eukaryotic protein phosphorylation sites. J. Mol. Biol. 294, 1351–1362.

Blom, N., Sicheritz-Pontén, T., Gupta, R., Gammeltoft, S., Brunak, S., 2004. Prediction of post-translational glycosylation and phosphorylation of proteins from the amino acid sequence. Proteomics 4, 1633–1649.

Bronsoms, S., Villanueva, J., Canals, F., Querol, E., Aviles, F.X., 2003. Analysis of the effect of potato carboxypeptidase inhibitor pro-sequence on the folding of the mature protein. Eur. J. Biochem. 270, 3641–3650.

Chang, J.Y., Canals, F., Schindler, P., Querol, E., Avilés, F.X., 1994. The disulfide folding pathway of potato carboxypeptidase inhibitor. J. Biol. Chem. 269, 22087–22094.

DeLano, W.L., 2002. The PyMOL Molecular Graphics System. DeLano Scientific, Palo Alto, CA, USA, <http://www.pymol.org>.

Dimitri, M., 1987. Descripción de plantas cultivadas. Encicl. Argentina Agric. y Jard. Tomo I.

Fear, G., Komarnytsky, S., Raskin, I., 2007. Protease inhibitors and their peptidomimetic derivatives as potential drugs. Pharmacol. Ther. 113, 354–368.

Fernández, D., Pallarès, I., Covaleda, G., Avilés, F.X., Vendrell, J., 2013. Metallocarboxypeptidases and their inhibitors: recent developments in biomedically relevant protein and organic ligands. Curr. Med. Chem. 20, 1595–1608.

Fischer, M., Kuckenberg, M., Kastilan, R., Muth, J., Gebhardt, C., 2014. Novel in vitro inhibitory functions of potato tuber proteinaceous inhibitors. Mol. Genet. Genomics. http://dx.doi.org/10.1007/s00438-014-0906-5.

García-Sáez, I., Reverter, D., Vendrell, J., Avilés, F.X., Coll, M., 1997. The three-dimensional structure of human procarboxypeptidase A2. Deciphering the basis of the inhibition, activation and intrinsic activity of the zymogen. EMBO J. 16, 6906–6913.

Gasteiger, E., Hoogland, C., Gattiker, A., Duvaud, S., Wilkins, M.R., Appel, R.D., Bairoch, A., 2005. The proteomics protocols handbook. In: Walker, J.M. (Ed.), The Proteomics Protocols Handbook. Humana Press, Totowa, NJ, pp. 571–607.

González, C., Neira, J., Ventura, S., Bronsoms, S., Rico, M., Avilés, F., 2003. Structure and dynamics of the potato carboxypeptidase inhibitor by 1H and 15N NMR. Proteins 50, 410–422.

Goodlad, R.A., Boulton, R., Playford, R.J., 1996. Comparison of the mitogenic activity of human epidermal growth factor I-53 and epidermal growth factor I-48 in vitro and in vivo. Clin. Sci. (London) 91, 503–507.

Gracy, J., Le-Nguyen, D., Gelly, J.-C., Kaas, Q., Heitz, A., Chiche, L., 2008. KNOTTIN: the knottin or inhibitor cystine knot scaffold in 2007. Nucleic Acids Res. 36, D314–D319.

Gregory, H., Thomas, C.E., Young, J.A., Willshire, I.R., Garner, A., 1988. The contribution of the C-terminal undecapeptide sequence of urogastrone-epidermal growth factor to its biological action. Regul. Pept. 22, 217–226. http://dx.doi.org/10.1016/0167-0115(88)90034-1.

Hass, G.M., Derr, J.E., 1979. Purification and characterization of the carboxypeptidase isoinhibitors from potatoes. Plant Physiol. 64, 1022–1028.

Jozic, D., Bourenkow, G., Bartunik, H., Scholze, H., Dive, V., Henrich, B., Huber, R., Bode, W., Maskos, K., 2002. Crystal structure of the dinuclear zinc aminopeptidase PepV from *Lactobacillus delbrueckii* unravels its preference for dipeptides. Structure 10, 1097–1106.

Kyte, J., Doolittle, R.F., 1982. A simple method for displaying the hydropathic character of a protein. J. Mol. Biol. 157, 105–132.

Larkin, M.A., Blackshields, G., Brown, N.P., Chenna, R., McGettigan, P.A., McWilliam, H., Valentin, F., Wallace, I.M., Wilm, A., Lopez, R., Thompson, J.D., Gibson, T.J., Higgins, D.G., 2007. Clustal W and Clustal X version 2.0. Bioinformatics 23, 2947–2948.

Lian, Q., Szarka, S.J., Ng, K.K.S., Wong, S.-L., 2003. Engineering of a staphylokinase-based fibrinolytic agent with antithrombotic activity and targeting capability toward thrombin-rich fibrin and plasma clots. J. Biol. Chem. 278, 26677–26686.

Marino-Buslje, C., Venhudová, G., Molina, M.A., Oliva, B., Jorba, X., Canals, F., Avilés, F.X., Querol, E., 2000. Contribution of C-tail residues of potato carboxypeptidase inhibitor to the binding to carboxypeptidase A. a mutagenesis analysis. Eur. J. Biochem. 267, 1502–1509.

Morrison, J.F., 1982. The slow-binding and slow, tight-binding inhibition of enzyme-catalysed reactions. Trends Biochem. Sci. 7, 102–105.

Obregon, W., Liggieri, C., Morcelle, S., Trejo, S., Aviles, F., Priolo, N., 2009. Biochemical and PMF MALDI-TOF analyses of two novel papain-like plant proteinases. Protein Pept. Lett. 16, 1323–1333.

Oliva, M.L.V., Sampaio, M.U., 2009. Action of plant proteinase inhibitors on enzymes of physiopathological importance. An. Acad. Bras. Cienc. 81, 615–621.

Pallarès, I., Fernández, D., Comellas-Bigler, M., Fernández-Recio, J., Ventura, S., Avilés, F.X., Bode, W., Vendrell, J., 2008. Direct interaction between a human digestive protease and the mucoadhesive poly(acrylic acid). Acta Crystallogr. D. Biol. Crystallogr. D64, 784–791.

Panosa, C., Tebar, F., Ferrer-Batallé, M., Fonge, H., Seno, M., Reilly, R.M., Massaguer, A., de Llorens, R., 2013. Development of an epidermal growth factor derivative with EGFR blocking activity. PLoS One 8. http://dx.doi.org/10.1371/journal.pone.0069325.

Playford, R.J., Marchbank, T., Calnan, D.P., Calam, J., Royston, P., Batten, J.J., Hansen, H.F., 1995. Epidermal growth factor is digested to smaller, less active forms in acidic gastric juice. Gastroenterology 108, 92–101. http://dx.doi.org/10.1016/0016-5085(95)90012-8.

Quesada, V., Ordóñez, G.R., Sánchez, L.M., Puente, X.S., López-Otín, C., 2009. The Degradome database: mammalian proteases and diseases of proteolysis. Nucleic Acids Res. 37, D239–D243.

Rawlings, N.D., Bateman, A., Barrett, A.J., 2012. MEROPS: the database of proteolytic enzymes, their substrates and inhibitors. Nucleic Acids Res. 40, D343–D350.

Rawlings, N.D., Waller, M., Barrett, A.J., Bateman, A., 2014. MEROPS: the database of proteolytic enzymes, their substrates and inhibitors. Nucleic Acids Res 42, D503–D509.

Rees, D.C., Lipscomb, W.N., 1982. Refined crystal structure of the potato inhibitor complex of carboxypeptidase A at 2.5 Å resolution. J. Mol. Biol. 160, 475–498.

Rose, G., Geselowitz, A., Lesser, G., Lee, R., Zehfus, M., 1985. Hydrophobicity of amino acid residues in globular proteins. Science 229, 834–838.

Schägger, H., 2006. Tricine-SDS-PAGE. Nat. Protoc. 1, 16–22.

Stothard, P., 2000. The sequence manipulation suite: javascript programs for analyzing and formatting protein and DNA sequences. Biotechniques 28, 1102–1104.

Tanco, S., Zhang, X., Morano, C., Avilés, F.X., Lorenzo, J., Fricker, L.D., 2010. Characterization of the substrate specificity of human carboxypeptidase A4 and implications for a role in extracellular peptide processing. J. Biol. Chem. 285, 18385–18396.

Tanco, S., Lorenzo, J., Garcia-Pardo, J., Degroeve, S., Martens, L., Aviles, F.X., Gevaert, K., Van Damme, P., 2013. Proteome-derived peptide libraries to study the substrate specificity profiles of carboxypeptidases. Mol. Cell. Proteomics 12, 2096–2110.

Turk, B., Turk, D., Turk, V., 2012. Protease signalling: the cutting edge. EMBO J. 31, 1630–1643.

Wang, X., Smith, P.L., Hsu, M.-Y., Ogletree, M.L., Schumacher, W.A., 2006. Murine model of ferric chloride-induced vena cava thrombosis : evidence for effect of potato carboxypeptidase inhibitor. J. Thromb. Haemost. 4, 403–410.

Zhang, H., Yao, Y., Yang, H., Wang, X., Kang, Z., Li, Y., Li, G., Wang, Y., 2012. Molecular dynamics and free energy studies on the carboxypeptidases complexed with peptide/small molecular inhibitor: mechanism for drug resistance. Insect Biochem. Mol. Biol. 42, 5835–5895.

Please cite this article in press as: Lufrano, D., et al. Biochemical characterization of a novel carboxypeptidase inhibitor from a variety of Andean potatoes. Phytochemistry (2015), http://dx.doi.org/10.1016/j.phytochem.2015.09.010